ACS APPLIED MATERIALS & INTERFACES

Research Article

www.acsami.org

Hydrogel Patterning by Diffusion through the Matrix and Subsequent Light-Triggered Chemical Immobilization

Zheyi Yi, Yu Zhang, Sujit Kootala, Jöns Hilborn, and Dmitri A. Ossipov*

Science for Life Laboratory, Department of Chemistry-Ångström Laboratory, Uppsala University, Uppsala, SE-75121 Uppsala, Sweden

Supporting Information

ABSTRACT: A novel approach to hyaluronic acid (HA) hydrogel with a chemical gradient of the matrix-linked bisphosphonate (BP) groups is presented. The method consists of two steps, including initial generation of physical gradient patterns of BPs by diffusion of BP acrylamide reagent into HA matrix carrying thiol groups and subsequent chemical immobilization of the BP groups by UV light-triggered thiol−ene addition reaction. This gradient hydrogel permits spatial three-dimensional regulation of secondary interactions of different molecules with the polymer matrix. In particular, graded amounts of cytochrome *c* (cyt *c*) were reversibly absorbed in the hydrogel, thus enabling the subsequent spatially controlled release of the therapeutic protein. The obtained patterned hydrogel acts also as a unique reactor in which peroxidase-catalyzed oxidation of a substrate is determined by spatial position of the enzyme (cyt *c*) in the matrix resulting in a range of product concentrations. As an example, matrix template-assisted oxidation of 3,3′,5,5′-tetarmethylbenzydine (TMB) in the presence of H_2O_2 occurs simultaneously at different rates within the gradient hydrogel. Moreover, calcium binding to the gradient HABP hydrogel reflects the pattern of immobilized BP groups eventually leading to the graded biomineralization of the matrix. This approach opens new possibilities for use of hydrogels as dynamic models for biologic three-dimensional structures such as extracellular matrix.

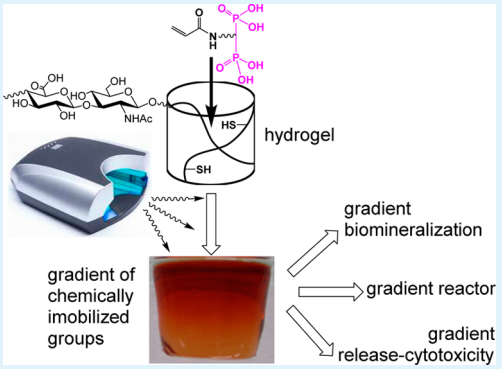

KEYWORDS: *hydrogel, chemical gradient, template synthesis, orthogonal reactions, hyaluronic acid*

INTRODUCTION

Hydrogels have been studied for applications in biological sensing, drug delivery, and tissue engineering because of their high water content, tissue-like elasticity, facile transport of nutrients, and waste.[1] Properties of hydrogels can be tuned by incorporation of appropriate ligands possessing distinct useful functionalities.[2] Conventional hydrogels are normally homogeneous and static, while native extracellular matrices (ECM) provide varying biochemical and biomechanical cues to the residing cells in space and time.[3,4] Recently, hydrogels with spatial heterogeneity[5−8] or the ability to undergo localized rapid change in cross-linking density in response to light[9−11] have emerged to explore the cells responses to dynamic alterations in 3D matrix properties. Inhomogeneous hydrogels presenting concentration gradients of immobilized factors are a particularly interesting class of materials in studies of chemotaxis,[12] morphogenesis,[13] and mechanotransduction[14] with respect to 3D-encapsulated cells. Such gradient hydrogels can substitute many homogeneous analogues with unique formulation for each individual gel (e.g., particular concentration of immobilized factor or cross-linking bond density). In addition, hydrogel implants with gradients properties, when placed on damaged tissues interfaces, can more ideally connect mechanically mismatched tissues such as bone−cartilage interfaces and dentino−-enamel junctions.[15]

To date, hydrogels incorporating chemical gradients were mainly prepared by a two-step approach in which concentration gradients of prepolymer solutions are formed first, followed by chemical photo-cross-linking affording a self-standing network.[16] Alternatively, homogeneous prepolymer solutions were exposed to variable amounts of UV light using either sliding[17] or gradient greyscale masks.[18] The majority of the methods rely on the same chemistry to both cross-link polymer chains and conjugate various ligands to the gel network. However, in these methods, gradient tethering of a ligand is accompanied by graded altering of cross-linking density which hampers the study of the effect of the ligand alone.[19] This shortcoming can be eliminated by applying orthogonal chemistries; one of each is used to form the hydrogel network, and a second chemistry is used to pattern in bioactive factors. Only a few examples exist, where UV-sensitive hydrogel structures were preformed physically or chemically first followed by gradient modification of the matrix using orthogonal photochemical reaction. Specifically, a varying amount of light was applied to different areas of hydrogels to break a portion of established hydrogel cross-links,[20] to create

Received: October 9, 2014
Accepted: December 31, 2014
Published: December 31, 2014

DOI: 10.1021/am506926w
ACS Appl. Mater. Interfaces 2015, 7, 1194−1206

Scheme 1. Schematic Representation of Preparation of Hyaluronic Acid Hydrogel with a Gradient Concentration of Bisphosphonate Ligands Covalently Attached to the Matrix[a]

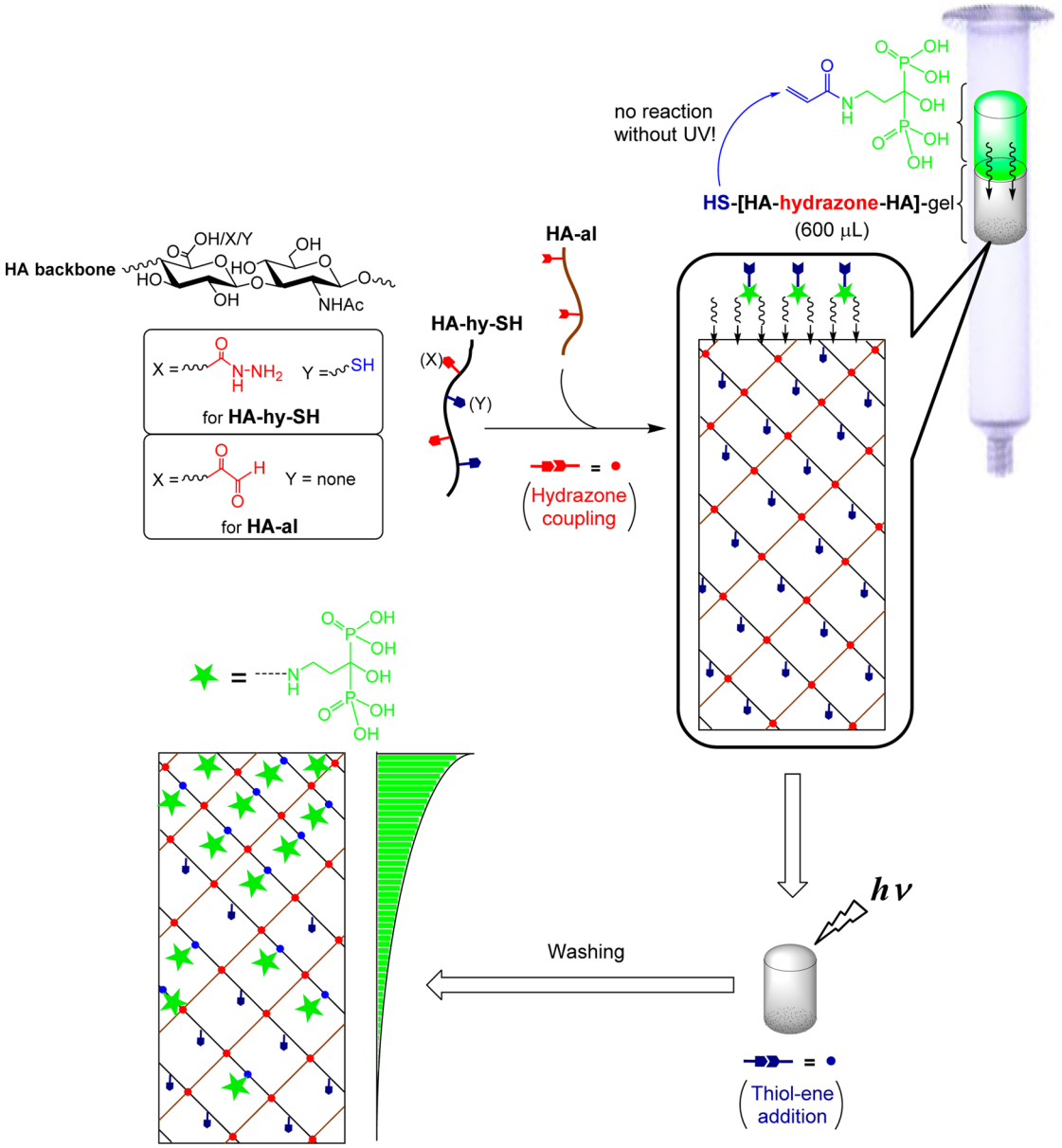

[a]The preparation is based on two consecutive chemoselective orthogonal reactions. The first hydrazone reaction is performed between soluble dually functionalized HA-hy-SH and HA-al derivatives affording the hydrogel material, while the second thiol−ene photoaddition reaction is performed after diffusion of BP-acrylamide reagent into the formed HA matrix.

additional interchain bonds,[21] or to covalently immobilize a ligand of interest (e.g., growth factor).[22] On the other hand, creating chemical gradients by grading the light exposure is always complicated by the fact that light intensity decreases with the increase of depth of light penetration into a hydrogel, limiting the technique to thin gel films.[23] In this study, we utilized diffusion of activatable molecules through a reactive matrix to establish first a physical molecular gradient which is followed by light-triggered chemical immobilization of the molecules. This method allows (i) independent control over homogeneous cross-linking and gradient bioconjugation using orthogonal chemistries, (ii) simple generation of long-range (centimeter range) stable chemical gradients by diffusion of molecules through a bulk polymer matrix, and (iii) generation of multigradient hydrogels. An important feature of this method is that the defusing molecules are not reactive until a physical gradient is established but can be rapidly, selectively, and efficiently linked after that. In this case development of a physical gradient is not perturbed by a chemical reaction occurring during the diffusion step as it was previously reported.[24]

In this work we used bisphosphonates (BPs) as ligands linked to hydrogel matrix with spatially graded concentration. BPs are antiosteoporotic drugs,[25] the action of which on bone resorbing cells, osteoclasts, is based on the high affinity of BPs to bind calcium ions.[26] The ability of BPs to bind to the mineral phase of bone has been exploited in bone targeting of radioisotopes,[27] anti-inflammatory and antineoplastic drugs,[28] cytokines and growth factors,[29] as well as polymeric therapeutics.[30] Recently, polymers containing bisphosphonate

DOI: 10.1021/am506926w
ACS Appl. Mater. Interfaces 2015, 7, 1194−1206

repeat units were found to function as powerful protein receptors.[31] On the basis of this fact, we previously compared hyaluronic acid (HA) hydrogels with and without covalently attached BP groups for binding and release of bone morphogenetic protein-2 (BMP-2), a growth factor that enhances bone regeneration.[32] We found that BP-functionalized HA hydrogel retains BMP-2, while the control HA hydrogel releases the growth factor over 2 days. We hypothesized therefore that a hydrogel with gradient distribution of covalently attached BP groups will also possess the spatially determined capacity to bind and release positively charged proteins. In this work, we examined this hypothesis by gradient anchoring of cytochrome *c* (cyt *c*) to HA matrix. Cyt *c*, a heme-containing metalloprotein,[33] can be entrapped in the mitochondrial membrane and act as an electron carrier in the respiratory chain. In addition, cyt *c* has also been identified as an important mediator of apoptosis through proteolytic cleavage on a wide range of cellular proteins.[34] The main objective of this work was, first, to demonstrate that hydrogels preformed with the residual thiol groups can be further patterned with bisphosphonate groups by diffusion of the appropriate "ene" ligands through the matrix followed by light-triggered chemical anchorage of the ligands. Because BP groups strongly interact with Ca^{2+} ions and basic proteins, another task was to demonstrate that the gradient pattern of BP groups permits graded mineralization of the obtained matrix as well as graded loading and release of a model protein, cyt *c*. Moreover, we exploited pro-apoptotic and peroxidase enzymatic properties of cyt *c* to show spatially differential cytotoxicity and biocatalytic activity of the obtained gradient HABP hydrogel.

RESULTS AND DISCUSSION

Gradient Patterning of Hydrogel by Diffusion. General scheme of preparation of a hydrogel with gradient concentration of the matrix-immobilized ligands is presented in Scheme 1. We have chosen hyaluronic acid (HA) as a matrix-forming macromolecule because HA is a natural component of ECM, while bisphosphonates (BPs) were gradually grafted to the matrix based on their protein-binding capacity.[31] Hydrazone coupling between hydrazide and aldehyde groups and photoinitiated thiol−ene addition reaction were considered to allow for independent control over the matrix formation and gradual conjugation of BP groups, respectively. The first step of matrix formation was performed by mixing aqueous solutions of HA-aldehyde (HA-al) and dually functional HA-hydrazide-thiol[35] (HA-hy-SH) derivatives and placing the combined solution to a syringe mold where the solution was transformed into a hydrazone hydrogel for 2 h. The matrix was formed as a result of hydrazone coupling between hydrazide and aldehyde groups leaving thiol functionalities unreacted and thus homogeneously linked to the obtained matrix. Second, an aqueous solution of BP-acrylamide and a radical initiator was applied from one plane side of the hydrogel for another 2 h. Diffusion of soluble components into the matrix resulted in a physical gradient of BP-acrylamide within the matrix. The final third step included exposure of the hydrogel to UV light, which initiated addition of the matrix thiol groups to soluble BP-acrylamide molecules and thus chemical fixation of the physical gradient. After the UV light treatment, the hydrogel was repeatedly washed with fresh 0.17 M NaCl solution in order to remove all matrix-unbound molecules.

The first evidence of gradient incorporation of BP groups along the direction of diffusion was obtained by observation of the shape of the hydrogel after final swelling in 0.17 M NaCl. Because the hydrogel of a 0.6 mL volume was formed in a 2 mL syringe, it had the shape of a cylinder with 9 mm height and 9 mm diameter. However, placing the initially cylindrical hydrogel in NaCl solution caused its nonuniform swelling along the principal rotation axis of the cylinder. Swelling was more prominent from the side where the hydrogel was in contact with the solution of BP-acrylamide than from the opposite side, and the swollen hydrogel had a shape of a truncated cone, the cut diameters of which were 11 and 9 mm, respectively (Figure S2a, Supporting Information). This result was expected assuming that ionized and highly negatively charged BP groups (four charges per group) should repel HA polymer chains from each other and increase their hydrodynamic volume. Consequently, a higher concentration of the attached BP groups should result in higher degree of swelling of the respective part of the HA hydrogel. To prove it further, we sectioned the hydrogel perpendicularly to the diffusion axis (Figure S2b, Supporting Information), and the amount of phosphorus in different sections was verified by SEM-energy-dispersive X-ray spectroscopy (SEM-EDXS, Table S1, Supporting Information). Consequently, the highest amount of phosphorus was detected in the first hydrogel section (numbering of the sections was performed from the hydrogel side where diffusion of BP-acrylamide started). The amount of linked phosphorus was gradually decreased in the following sections, and in the last section it was 8 times less than in the first one.

The presented method of generation of a chemically fixed gradient of hydrogel matrix-appended ligands requires hydrogel setting, diffusion of a ligand through the matrix, and finally UV-light-mediated ligand attachment. The total time required for these steps is sufficiently long (4 h with our hydrogel geometries) to allow 3D cell encapsulation and consequent hydrogel patterning without affecting cell viability. This limitation can be overcome by postfabrication insertion of cells into a hydrogel analogously to cell seeding to porous scaffolds. The low penetration ability of cells into scaffolds can restrict this technique to only 2D seeding of cells. The missing third dimension can be added using different additive manufacturing techniques.

Comparison of Gradient Hydrogel with Its Homogeneous Analogues. To systematically investigate the mechanistic aspects of the formation of gradient of chemically attached BP groups in HA hydrogel, we measured the binding of cytochrome *c* (cyt *c*) to different macroscopic hydrogels. Cyt *c* is a small (M_w = 12 327, hydrodynamic diameter of 3.5 nm), highly water soluble, fluorescent, and positively charged (net charge of +9.3 at neutral pH) heme protein[36] allowing for easy detection of BP groups to which the protein molecules should be electrostatically attracted. We first compared the gradient hydrogel with its two homogeneous analogues, i.e., the pure HA hydrogel and the HA hydrogel in which BP groups were linked to the matrix homogeneously (HABP hydrogel). Preparation of the homogeneous hydrogels consisted of the same three steps utilized for the preparation of the gradient hydrogel except that the first diffusion step was omitted from the preparation (Scheme 2). The same amount of BP-acrylamide used in the diffusion step (9 mg) was also present in the starting solution of HA-aldehyde derivative in order to afford homogeneous HABP hydrogel.

A striking difference in cyt *c* loading capacity of the hydrogels was observed already during visual examination of the

DOI: 10.1021/am506926w
ACS Appl. Mater. Interfaces 2015, 7, 1194−1206

Scheme 2. Preparation of Homogeneous HA hydrogels with or without Matrix-Linked BP Groups in Comparison with the Preparation of Gradient HABP Hydrogel[a]

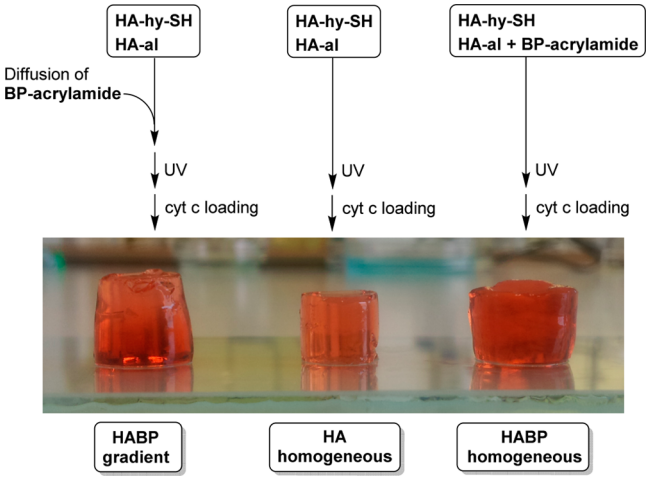

[a]All hydrogels were loaded with cyt *c* for visualization.

hydrogels after the protein loading. Thus, control HA hydrogel lacking BP groups was homogeneously laden with the protein to the lowest extent, while control HABP hydrogel showed maximal and homogeneous entrapment of cyt *c*. Importantly, the hydrogel that was in contact with the solution of BP-acrylamide for 2 h showed intermediate loading with the gradient distribution of cyt *c* concentration along the *Z* axis (vertical in Scheme 2). While the fluorescence intensity of the upper part of gradient HABP gel resembled the one for the homogeneous HA gel, the bottom part was more similar to the homogeneous HABP gel. Second, the hydrogels had different swelling characteristics. Homogeneous HABP hydrogel was swollen to a greater extent than HA hydrogel, although they were both of cylindrical shape. A gradual change of swelling along the *Z* axis was observed for the hydrogel that was exposed from one side to BP-acrylamide solution. The cone-type shape of this hydrogel can be explained by the gradient distribution of the BP groups attached to the HA matrix with the highest concentration of BPs in the hydrogel part of the larger diameter.

Gradient HABP hydrogel was found to be mechanically stronger than its homogeneous analogues both before and after loading with cyt *c* (Table 1). The average G' was 2577 ± 175 Pa for the gradient hydrogel, while homogeneous hydrogels with and without attached BP groups showed lower elasticity: G' = 1897 ± 170 Pa for HA hydrogel and G' = 1690 ± 85 Pa for the HABP analogue. The same trend remained after loading of cyt *c*, albeit elastic moduli decreased slightly for all types of hydrogels. The reason for the higher elastic properties of the gradient hydrogels in comparison with the homogeneous analogues is unclear. It may relate to the anisotropic nature of the gradient hydrogel. For example, the elastic modulus of composite poly(ethylene glycol)/polycaprolactone (PEG/PCL) hydrogels measured along the parallel aligned PCL fibers was higher as compared with PEG/PCL hydrogels with the irregular arrangement of the PCL fibers.[37]

Table 1. Mechanical Properties of Homogeneous HA Hydrogels with or without Matrix-Linked BP Groups in Comparison with the Gradient HABP Hydrogel

	G', Pa	
hydrogel type	before loading of cyt *c*	after loading of cyt *c*
gradient HABP	2577 ± 175	2297 ± 167
homogeneous HA	1897 ± 170	1582 ± 78
homogeneous HABP	1690 ± 85	1357 ± 205

The protein-laden hydrogels were subjected to treatment by hyaluronidase, the enzyme that degrades HA, in order to quantitatively determine the loading capacity of all three hydrogels. The amount of cyt *c* in feeding solution was 5 mg for each hydrogel (0.6 mL of gels was incubated in 5 mL of phosphate-buffered saline (PBS) containing the protein at 1 mg/mL concentration). Thus, the polymer content of the hydrogel was in excess over the amount of the protein applied (molar ratio of HA carboxylic groups to total cyt *c* amino groups was 3.23). After 5 days of incubation, the amount of cyt *c* left in the feeding solution was 4.38 ± 0.03 (87.6 ± 0.6%), 2.19 ± 0.08 (43.8 ± 1.6%), and 3.28 ± 0.15 mg (65.6 ± 3.0%) for homogeneous HA, homogeneous HABP, and gradient HABP hydrogels, respectively. Degradation of the cyt *c* loaded hydrogels led to the release of the free protein in the following amounts: 0.77 ± 0.02 (15.4 ± 0.4%), 2.45 ± 0.04 (49.0 ± 0.8%), and 1.98 ± 0.07 mg (39.6 ± 1.4%) for homogeneous HA, homogeneous HABP, and gradient HABP hydrogels, respectively. Thus, cyt *c* loading that can be obtained from the protein depletion in the feeding solutions is corroborating with the measurements of cyt *c* in the hydrogels digests.

Correlation of the Amount of the Absorbed Cytochrome *c* with the Amount of HA Matrix-Linked BP Groups. It was evident that the amount of cyt *c* that can be loaded into HA hydrogel is directly proportional to the amount of the matrix-linked BP groups. We studied the role of hydrogel charge in protein encapsulation using a series of homogeneous bulk polyelectrolyte networks with different BP contents. For that we varied the amount of BP-acrylamide from 0 to 15 mg in the initial liquid formulation composed also of HA-hy-SH and HA-al precursors (homogeneous gels in Scheme 2). The volume of the resulting hydrogel after swelling in PBS was found to scale quantitatively with the amount of BP reagent included in the synthesis (Table S2, Supporting Information) which was indicative for incorporation of more negative charge into the matrix. Loading of cyt *c* resulted in the hydrogel volume decrease as a result of polyelectrolyte interactions between the cationic protein and the negatively charged matrix (Table S2, Supporting Information).[38] Relative network contraction was slightly larger for the pure HA-based hydrogel (25%) as compared to the BP-immobilized analogues (17% in average). Interestingly, however, the hydrogel prepared with the highest amount of BP-acrylamide (15 mg) changed its volume to the least extent (8.5%) after cyt *c* loading. This observation was in corroboration with the mass of the loaded protein. It increased linearly with the increase of the BP-acrylamide feeding amount from 0 to 6 mg (Figure S3a, Supporting Information). It was noteworthy, however, that the increase of the protein loading leveled during further increase of the applied amount of BP reagent from 9 to 15 mg. Similarly, the calculated concentration of the loaded cyt *c* in the hydrogels was linearly proportional to the amount of BP-acrylamide used in the synthesis in the range from 0 to 6 mg followed by its stabilization in the range between 6 and 9 mg (Figure S3b, Supporting Information). In particular, pure HA hydrogel could accommodate cyt *c* at a concentration of 1.8 mg/mL. By

DOI: 10.1021/am506926w
ACS Appl. Mater. Interfaces 2015, 7, 1194−1206

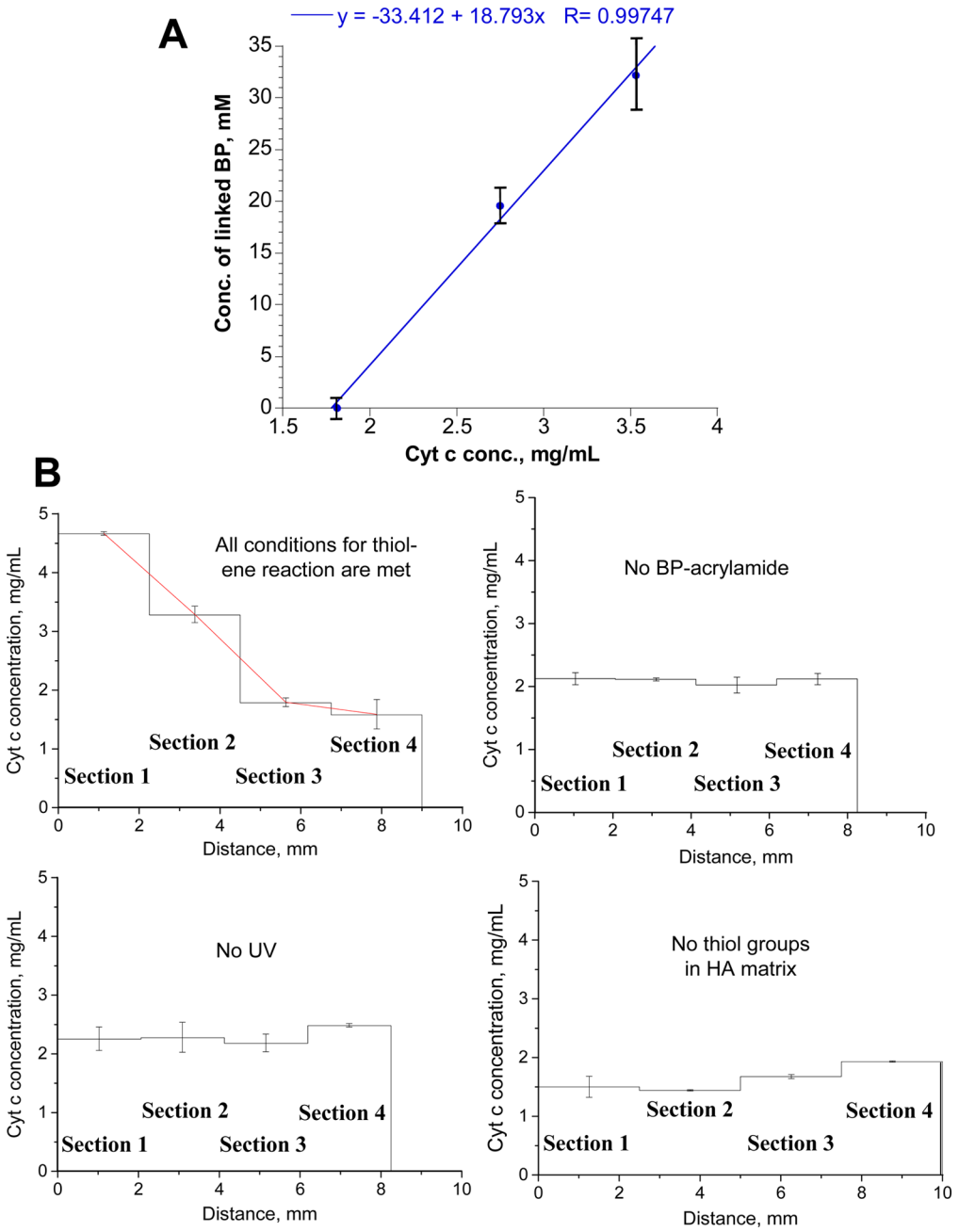

Figure 1. (a) Correlation between the concentration of matrix-immobilized BP groups (mM) and the concentration of cyt *c* absorbed in homogeneous HA hydrogel (mg/mL). (b) Distribution of loaded cyt *c* in the hydrogels patterned by diffusion under different conditions (depicted as average for $n = 3$, error bars represent standard deviation).

incorporation of BP groups into HA matrix, one could almost double the protein loading capacity of HA hydrogel achieving maximal cyt *c* concentration in the hydrogel at 3.5 mg/mL. Active uptake of cyt *c* and its condensation in the matrix is evident when comparing the concentrations of the encapsulated protein (1.8−3.5 mg/mL) with its concentration in the feeding solution (1 mg/mL).

Clearly, the accommodation of cyt *c* in the hydrogels should be hindered by the excluded volume and cross-inking density but effectively driven by electrostatic attraction of the protein by the matrix with the increasing negative charge. In this work, incorporation of higher amounts of negatively charged BP groups into HA matrix of the same initial density of hydrazone cross-links should result both in a decrease of the actual cross-linking density due to the hydrogel swelling effect as well as in an increase of the protein−matrix binding. The observation of saturation of the protein loading capacity of the hydrogels prepared with the increasing amount of BP-acrylamide indicates that the reagent immobilization within the thiol-presenting matrix via thiol−ene addition reaction can be terminated at a certain stage. Typically one thiol group can add across one vinyl monomer via a step-growth mechanism.[39] However, carbon radical propagation was also observed after initial thiyl radical addition to acrylate monomers leading to a chain growth.[40] In our series of homogeneous hydrogels, molar ratios of BP monomers to thiol groups were 0, 3.3, 6.7, 10, and 16.7, assuming only oligomerization of the BP monomers. On the other hand, it has been reported that BP groups may terminate

DOI: 10.1021/am506926w
ACS Appl. Mater. Interfaces 2015, 7, 1194−1206

free radicals during the reaction.[41] Importantly, hydrogel matrix itself should impose structural constraints for the "grafting-from" type of homopolymerization occurring inside the matrix. To the best of our knowledge, there have not been reports on polymerization reactions performed in the interior of a hydrogel matrix and initiated from the matrix-bound chain transfer agent.

In conclusion, on the basis of the above results, we tentatively assumed that 100% of BP−acrylamide can be immobilized to the HA matrix when the initial feeding amount of the reagent was not exceeding a certain level (6−9 mg). Consequently, within the linear region of correlation between the reagent feeding amount and the amount of the absorbed protein, we could approximately assess the amount of the matrix-immobilized BP groups from the amount of the loaded cyt *c* (Figure 1a).

Conditions of Thiol−Ene Photoinitiated Addition Reaction Are Essential in Preparation of Gradient Hydrogel. In order to confirm the mechanism of generation of a gradient of BP groups chemically linked to the HA matrix and presented in Scheme 1, the conditions of the thiol−ene immobilization reaction were varied and the obtained hydrogels were investigated by loading of cyt *c* (Scheme 3). Theoretically,

Scheme 3. Preparation of Patterned Hydrogels by Diffusion under Different Conditions[a]

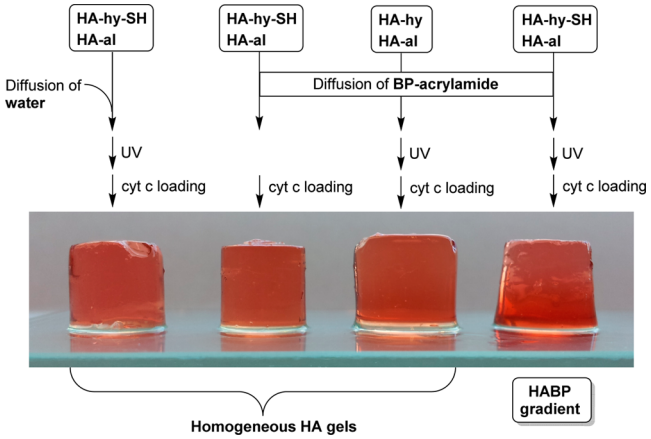

[a]Gradient HABP hydrogel can only be prepared under the conditions of thiol−ene photoinitiated addition reaction. All hydrogels were loaded with cyt *c* for visualization.

a radical is generated from the initiator molecule upon absorption of a photon of UV light and then transferred to a thiol group. The obtained thiyl radical is subsequently added across the double bond of BP-acrylamide that has been already diffused into the matrix resulting in chemical fixation of the physical gradient of BP-acrylamide molecules in the matrix. Therefore, BP-acrylamide, thiol, or UV light was excluded from the standard preparation procedure for the gradient hydrogel. The corresponding hydrogels were designated as noBP, noSH, and noUV HA hydrogels. The rest of the conditions were maintained identical. To prepare hydrazone hydrogel lacking thiol groups, HA-hy-SH derivative was substituted with its HA-hydrazide (HA-hy) analog possessing the same amount of hydrazide groups. Images of the hydrogels were analyzed using ImageJ software. Visual examination as well as image analysis of noBP, noUV, and noSH HA hydrogels after loading of cyt *c* (Figure S4, Supporting Information) revealed no gradient distribution of the protein as compared with the hydrogel for which all the conditions for BP immobilization by the thiol−ene photoaddition reaction were met. In particular, along the diffusion axis, the color values for noBP, noUV, and noSH HA hydrogels were around 82.7 ± 15.0, 70.2 ± 4.1, and 72.4 ± 8.2, respectively. On the contrary, the hydrogel patterned by diffusion of BP-acrylamide through the thiol-presenting matrix followed by exposure of the hydrogel to UV light exhibited nearly linear color change from 94.0 to 25.2.

Cyt *c* depletion in the feeding solutions revealed that 0.655 ± 0.004 (13.1 ± 0.1%) and 0.47 ± 0.05 mg (9.4 ± 0.9%) of the protein were loaded into noBP and noUV HA hydrogels, respectively. These values are very close to the similarly determined cyt *c* loading capacity of the homogeneous HA hydrogel (12.4 ± 0.7%). On the other hand, 1.056 ± 0.072 mg (21.1 ± 1.4%) of cyt *c* was loaded into the hydrogel prepared without the residual thiol groups. This can be attributed to the decreased cross-linking density of the hydrogel prepared from HA-hydrazide (HA-hy) derivative as compared to the cross-linking density of the hydrogels derived from the dually functional HA-hydrazide-thiol (HA-hy-SH). Apart from hydrazone cross-linking, additional disulfide cross-linking of HA chains can take place with the thiol-containing HA.[35] Consequently, absorption of cyt *c* by the less cross-linked matrix is expected to proceed more effectively.

Gradient HABP hydrogel and noBP, noUV, and noSH HA hydrogels were sectioned along the diffusion axis into four parts of the same thickness (numbering of the sections was done starting from the diffusion side), and the hydrogel sections were degraded by hyaluronidase to free the encapsulated cyt *c*. Quantitative determination of the immobilized cyt *c* in the sections of the examined hydrogels (Figure 1b) thus permitted assessment of the amount of the attached BP groups along the diffusion axis. First, the average concentration of cyt *c* was not varying among the sections of the hydrogels that were patterned by diffusion under the compromised conditions for the thiol−ene photoaddition reaction. Specifically, noBP, noUV, and noSH HA hydrogels exhibited a uniform distribution of the encapsulated cyt *c* with an average concentration of 2.10 ± 0.10, 2.30 ± 0.15, and 1.64 ± 0.25 mg/mL, respectively. The fact that noBP and no UV hydrogels were characterized by slightly higher cyt *c* loading in comparison with that for the homogeneous HA hydrogel (1.81 ± 0.05 in Table S2, Supporting Information) can be attributed to the altering of the hydrogel setting conditions (i.e., inclusion of the diffusion step into the preparation procedure). Importantly, the protein distributions within noUV and noBP hydrogels were homogeneous and equal. It indicates that despite the diffusion of BP-acrylamide into the matrix, no stable gradient of BP ligands could be created without UV light. Finally, the actual concentration of cyt *c* loaded in noSH HA hydrogel (1.64 ± 0.25 mg/mL) appeared to be slightly less than in the homogeneous HA hydrogel. As mentioned above, the cross-linking density of noSH HA hydrogel should be less than that for the homogeneous HA hydrogel, resulting in both higher hydrogel swelling (volume) and higher absolute protein loading (mass). The resulting protein concentration may decrease in this case.

When all the conditions for thiol−ene immobilization reaction were met during the preparation of the diffusion-patterned hydrogel, the sections of the obtained hydrogel were characterized by noneven distribution of the encapsulated cyt *c* (Figure 1b). The concentration of cyt *c* in sections 1, 2, 3, and 4

DOI: 10.1021/am506926w
ACS Appl. Mater. Interfaces 2015, 7, 1194−1206

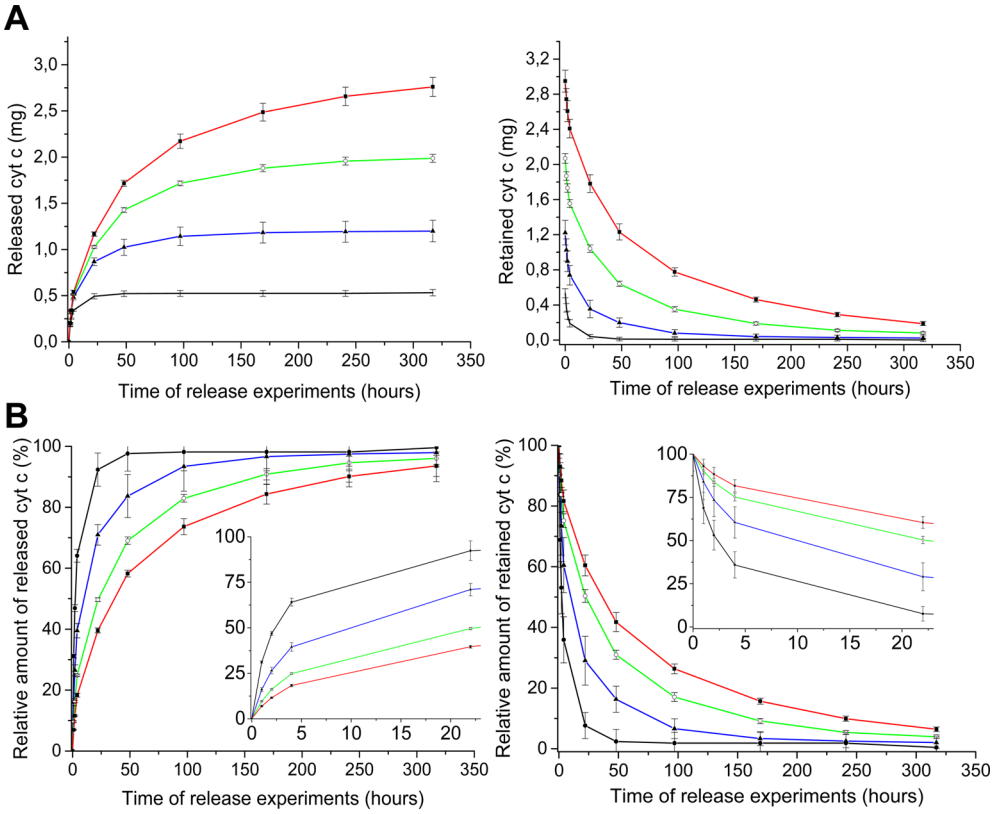

Figure 2. (a) Absolute amounts of cyt *c* that were released from the homogeneous hydrogels (left) and retained in them (right). (b) Relative amount of cyt *c* that was released from the homogeneous hydrogels (left) and retained in them (right). Homogeneous hydrogels were prepared without BP-acrylamide (no linked BPs, black curves) as well as with 3 (~18 mM of linked BPs, blue curves), 6 (~33 mM of linked BPs green curves), and 9 mg (red curves) of BP-acrylamide.

of the hydrogel was 4.66 ± 0.03, 3.28 ± 0.14, 1.79 ± 0.08, and 1.58 ± 0.25 mg/mL respectively. It can be seen that a stable protein gradient was created in sections 1−3 of the hydrogel, while there was almost no difference in cyt *c* loading in sections 3 and 4. On the basis of this data we could conclude that the whole range of BP functionalization of HA matrix from maximal 32 to 0 mM (Figure 1a) was established in the corresponding sections of the hydrogel. It is important to note that the diffusion of BP-acrylamide into a thiol-presenting matrix followed by thiol−ene coupling of the BP reagent should result in the thiol groups consumption for BP functionalization on one side of the hydrogel and for disulfide cross-linking on the other side of the hydrogel (Scheme 1). These two events should have a concerted effect on cyt *c* loading, i.e., the protein loading should increase with the increase of BP functionalization as well as with the decrease of disulfide cross-linking. Consequently, this might give rise to a higher difference in cyt *c* loading than was observed between the homogeneous HA and HABP hydrogels (1.8 and 3.5 mg/mL respectively). The observed difference between 1.6 and 4.7 mg/mL of cyt *c* loading confirmed this assumption. It is important to note that the thiol−ene addition reaction served only for chemical immobilization of the created physical gradient. Formation of the physical gradient itself should depend on the diffusion process and can be controlled by such parameters as the concentration of a ligand (BP-acrylamide in this case), geometry of the hydrogel, and geometry of the interface between the hydrogel and the ligand solution.

Spatially Patterned Drug Delivery by the Gradient HABP Hydrogel. After confirmation of gradient chemical patterning of HA with BP groups and subsequent graded loading of the resulting hydrogel with cyt *c*, we sought to demonstrate the usefulness of gradient protein loading in the hydrogel matrix. Considering the pro-apoptotic effect of cyt *c*, the HABP hydrogel loaded with graded amounts of the protein may function as a local depot for the spatially patterned delivery of the therapeutic to cancer cells. In other words, the hydrogel should exhibit a range of toxicities with extreme values spatially localized in the opposite parts of the hydrogel depot. To evaluate the retention effect of BP groups, we first studied the release of cyt *c* that was loaded into homogeneous hydrogels of various contents of the matrix-linked BP groups. Larger absolute amounts of cyt *c* were released from the homogeneous hydrogels characterized by a higher degree of BP functionalization (Figure 2a, left). This result was expected because initial loading of cyt *c* into the hydrogels was directly proportional to the amount of the matrix-linked BP groups (Figure 1a). On the other hand, the same reason for the exceptional binding affinity of bisphosphonated HA to the protein should also result in higher retention of the cargo in the hydrogels with a higher degree of BP functionalization (Figure 2a, right). We therefore evaluated the relative release of cyt *c*, i.e., the ratio of the amount of cyt *c* released from a hydrogel to the whole amount of the protein loaded into the hydrogel. It was found that the fastest release was from the pure HA hydrogel with 92.4 ± 5.4% of the protein released already after 22 h (Figure 2b, left). The rate of release was subsequently slower with the increase of BP content in the hydrogel. It should be noted, however, that the increase of the protein retention slowed down from the hydrogels prepared with 9 mg of BP-acrylamide. For example,

DOI: 10.1021/am506926w
ACS Appl. Mater. Interfaces 2015, 7, 1194−1206

after 22 h of the release experiments, 71.0 ± 3.3%, 49.7 ± 0.6%, and 39.7 ± 0.8% of cyt *c* were released from the hydrogels prepared with 3, 6, and 9 mg of BP-acrylamide, respectively. It confirmed our previous assumption about a certain limit of BP functionalization that must exist for such an "in-hydrogel" homopolymerization from the matrix-bound thiol groups.

Comparison of concentration of the loaded protein (1.8−3.5 mg/mL or 0.15−0.29 mM) with the concentration of the matrix-linked BP groups (0−33 mM) implies that from 0 to ∼115 BP groups corresponded to one cyt *c* molecule in the hydrogels loaded by swelling in the protein solution. These corresponded to the molar ratios of BP groups and total amino groups of cyt *c* from 0 to ∼5 (a molecule of cyt *c* contains 13 carboxyl groups and 23 amino groups[42]). Thus, the protein/matrix BP molar ratio during the protein loading spanned from the infinite excess of the protein to a stoichiometric balance between the oppositely charged groups (four negative charges of bisphosphonate per one positive charge of the amino group). Clearly, a higher feeding amount of cyt *c* is preferable to achieve better differentiation in the protein loading between the hydrogels with different binding affinities. On the other hand, equilibrium loading of a protein is provided by the used encapsulation method (hydrogel swelling in the protein solution for 5 days). In this concentration region it was possible to accurately tune the retention (release) of the protein, while complete protein retention is envisaged at the concentrations of the matrix-linked BP groups far exceeding the concentration of the encapsulated protein. This situation was realized in our previous studies when the in situ encapsulated BMP-2 was sequestered in the HABP matrix.[32] An alternative manner of regulation of the retention (release) of a protein of interest in HA hydrogel can be through in situ encapsulation of the protein in the matrix formed from different amounts of soluble and cross-linkable HA-BP derivative (such as dually modified HA-hydrazide-bisphosphonate[32,43]). The obtained results unequivocally showed that both loading of the protein and its release can be finely controlled by the amount of the matrix-attached BP groups.[44]

On the basis of the results of cyt *c* release from the homogeneous hydrogels, we then investigated the release of the protein from different sections of the gradient HABP hydrogel. For this purpose, the sections of the hydrogel were incubated for 24 h in PBS and the amount of the released protein was measured by UV−vis spectrophotometry (Figure 3a). As expected, the amount of the released cytochrome *c* was maximal (0.29 ± 0.05 mg) from the first section with the highest protein loading after 24 h of incubation in PBS. The following sections, which were characterized by progressively decreasing protein loading, released 0.19 ± 0.01, 0.13 ± 0.02, and 0.083 ± 0.002 mg of cyt *c*, respectively. These amounts were in accord with the released amounts of cyt *c* from the homogeneous hydrogels of the corresponding loadings. Analogously to the homogeneous hydrogels with increasing amount of matrix-linked BP groups, the section of the gradient hydrogel with the lowest content of BP groups was characterized by the lowest amount of the retained protein (55.0 ± 8.7%) and the protein retention effect increased with the increase of BP content along the diffusion axis of the gradient hydrogel. The section of the gradient hydrogel with the highest content of BP groups retained 72.7 ± 8.9% of the protein.

Next, we investigated whether gradient HABP hydrogel with loaded cyt *c* could induce graded apoptosis of cancer cells. To

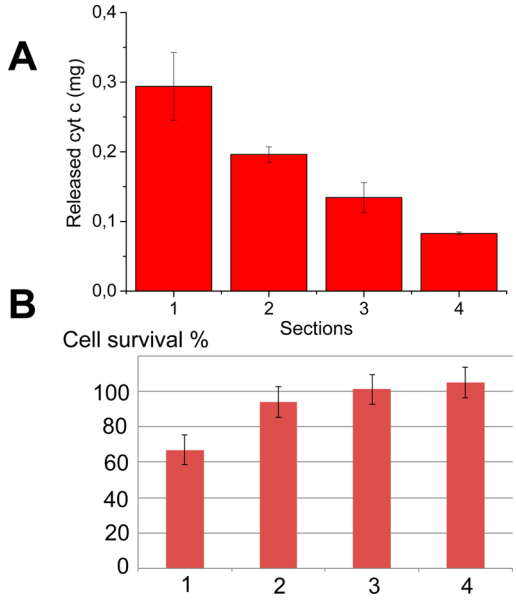

Figure 3. (a) Amount of cyt *c* released from the sections of the gradient HABP hydrogel. (b) Viability of MCF-7 cells cultured for 24 h in 5% DMEM that also served as a release medium for different sections of cyt *c* loaded gradient HABP hydrogel (depicted as average for $n = 3$, error bars represent standard deviation). Hydrogel sections were placed onto cell culture inserts. Numbering of the sections starts from the hydrogel side with highest loading of cyt *c*.

this goal, different sections of the gradient HABP hydrogel were placed in separate cell culture inserts and MCF 7 cells were cultured on the bottom of plate wells for 24 h. This experimental setup provided transport of the released molecules from the hydrogel sections in the insets to the cells through the inset membrane. After 24 h of incubation at 37 °C we found that a reduction in the viability of MCF 7 cells was corroborated with the amount of cyt *c* released from the sections of the hydrogel (Figure 3b). In fact, only in section 1, when the cells were exposed to the maximal cyt *c* concentration of 0.19 mg/mL (15.7 μM) during the incubation period, we could observe cytotoxicity effect (63%). In other sections, viability of MCF 7 cells was not statistically different and close to 100%. It should be noted that the cytotoxic effect of free cyt *c* was detected starting from a concentration of 0.1 mg/mL and higher (Figure S6, Supporting Information). Because sections 2−4 released cyt *c* at concentrations of 0.12 mg/mL and lower, it was expected that the cells exposed to these sections should have 100% survival. Thus, these experiments confirmed our assumption that hydrogels with graded loading of a drug can exhibit spatially patterned cytotoxicity.

Gradient Biomineralization of the BP-Patterned Hydrogel. Previously we have shown that BP functionalization of HA hydrogel had a profound effect on the mineralization properties of the resultant hydrogel.[43] Upon incubation of the hydrogel in mineralization medium, BP groups chelate Ca^{2+} ions with the formation of Ca^{2+}-bridged BP clusters within the HA matrix. These clusters, in turn, serve as nucleation points for the deposition of calcium phosphate mineral in the form of nanoparticles that become embedded inside the organic matrix. On the contrary, pure HA-based hydrogel has much less mineralization capacity. Consequently, hydrogel with a gradient distribution of the matrix-linked BP groups presents a unique material, which will evolve in an anisotropic manner when

DOI: 10.1021/am506926w
ACS Appl. Mater. Interfaces 2015, 7, 1194−1206

placed in an appropriate complex environment (in vivo). Mineralization in hydrogels is important to render these materials suitable in bone tissue regeneration.[45] On the other hand, bone itself has a functionally graded structure from the surface cortical bone toward the inner cancelous bone. Therefore, there should be of interest to design a hydrogel implant that allow graded hydroxyapatite deposition in the hydrogel.

To test our hypothesis, hydrogel patterned by diffusion of BP-acrylamide followed by UV treatment and repeated incubation in 0.17 M NaCl was finally placed into simulated body fluid (SBF) for different amounts of time (1 h, 1 day, or 7 days). The hydrogel was subsequently sectioned into four parts of the same thickness, and the calcium content of the sections was examined by spectrophotometric measurement of Ca^{2+} complex with Arsenazo III dye. The section of the hydrogel that was exposed to BP-acrylamide solution was numbered first, and then numbering was continued in the direction of diffusion. As expected, the amount of Ca^{2+} decreased from section 1 to section 4 of the hydrogels after mineralization for all periods of time studied (Figure 4). A detectable difference in mineralization pattern between the sections was already observed after 1 h of the hydrogel incubation in SBF. Moreover, there was an uneven increase in Ca^{2+} content over the first day of incubation. Figure 4 reveals that the extent of mineralization and the rate of mineralization during the first day was the highest for section of 1 of the hydrogel containing the highest amount of BP groups (i.e., 32 mM based on our cyt *c* binding studies). In particular, the extent of mineralization of section 1 was 14.37 ± 0.17 and 14.64 ± 0.64 μg after 1 and 7 days, respectively. Both the extent of mineralization and the rate of mineralization during the first day progressively decrease from section 1 to section 4. An increase in Ca^{2+} content of sections 1−3 was more noticeable over the first 24 h than during another 6 days of mineralization. Section 4 was expected to present HA matrix without the attached BP group. Consequently, the Ca^{2+} content of section 4 did not change much during the whole time of incubation and maintained at the lowest observed level (around 4.3 μg). Hence, the obtained data unequivocally confirmed the gradient biomineralization pattern of the hydrogel with the graded amounts of the matrix-linked BP groups. Essentially, the presented gradient hydrogel may generally function as a "reactor", different compartments of which may impose different control for the matrix-templated growth of inorganic nanoparticles. To date, such possibility of using gradient hydrogels as anisotropic templates for performing various inorganic and organic reactions remained virtually untapped.

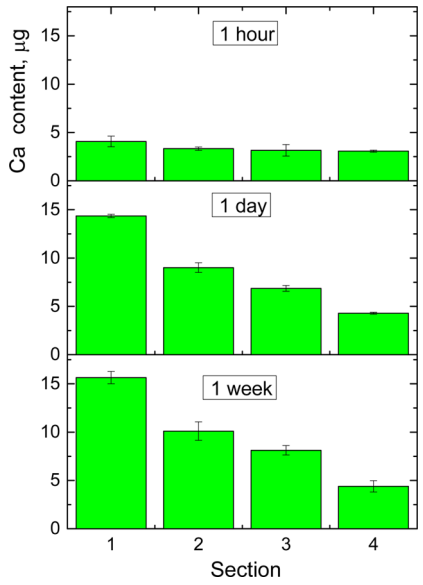

Figure 4. Calcium contents in different sections of BP-patterned hydrogels after hydrogels incubation in SBF for 1 h, 1 day, or 1 week (depicted as average for n = 3; error bars represent standard deviation). Numbering of the sections starts from the hydrogel side that has been exposed to the solution of BP-acrylamide during the hydrogel patterning.

Control of Biocatalysis through Graded Immobilization of Enzyme in Hydrogel Matrix. Strong interactions that are established between BP groups of HA matrix and cyt *c* can be advantageous for enzyme immobilization inside hydrogels. Such immobilization enables reuse of the enzyme, enhances its stability, and may improve its catalytic activity. In the case with gradient HABP hydrogel, it may allow for the graded generation of products of enzymatic reaction inside the matrix. Site-specific drug delivery was addressed previously by providing a flow of a prodrug through a biocatalytic surface with adhered cells.[46] The cells adhered to pristine surface located "downstream" of the biocatalytic one had higher viability because conversion of the prodrug to the cytotoxic drug was only possible at the site with the immobilized enzyme. In this work we evaluated cyt *c* integrity within the hydrogels and assessed its known peroxidase activity toward a widely used chromogenic substrate, 3,3′,5,5′-tetramethylbenzidine (TMB), after graded encapsulation of the protein. For this purpose, the gradient HABP hydrogel (0.6 mL) was equilibrated in 5 mL of cyt *c* solution in PBS (1 mg/mL) for 5 days and subsequently sectioned along the diffusion axis to obtain a thin (1 mm) film from the middle of the hydrogel truncated cone (Figure S8, Supporting Information). The obtained gel section was then loaded with TMB by incubation in 5 mL of the substrate solution (0.2 mg/mL). Next, the gradient hydrogel film was quickly rinsed by distilled water and placed into a Petri dish, and 10 mL of 5.9 mM H_2O_2 solution was added. Figure 5 shows photographic snapshots of the hydrogel film after addition of the oxidizing agent. Within several minutes after the beginning of diffusion of hydrogen peroxide into the hydrogel its color started to change to blue, passed through a green stage, and finally became yellow. This observation indicated two-electron oxidation of TMB with the formation of intermediate

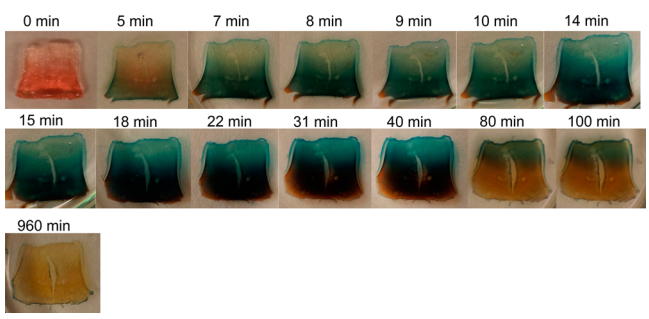

Figure 5. Oxidation of TMB in the HABP hydrogel loaded with graded amounts of cyt *c*. A section of the gradient hydrogel was incubated first in solution of TMB for 2 h followed by placing the hydrogel into H_2O_2 solution. The hydrogel was photographed before oxidation (image at 0 min) and after certain intervals of time during the treatment in H_2O_2 solution.

DOI: 10.1021/am506926w
ACS Appl. Mater. Interfaces 2015, 7, 1194−1206

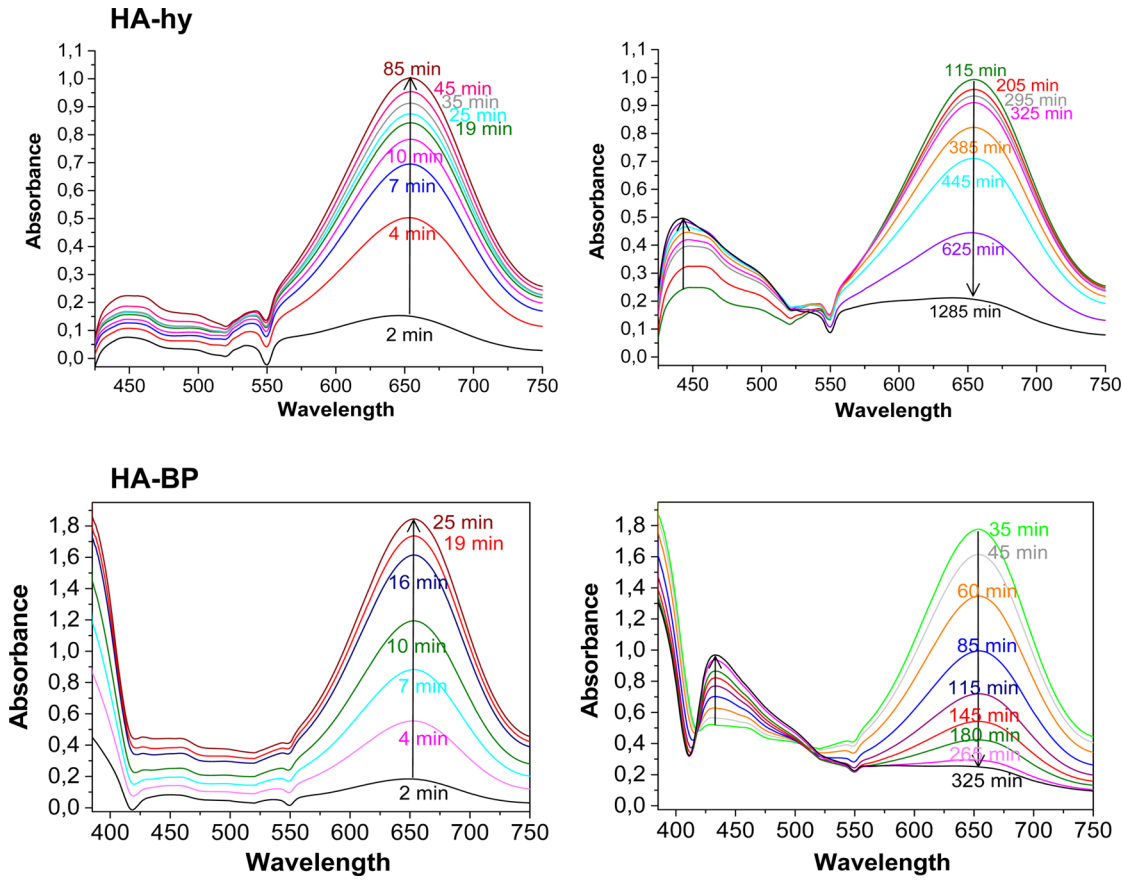

Figure 6. UV−vis spectra of oxidation of TMB by cyt c/H_2O_2 in solution containing either HA-hy (top) or HA-BP derivatives (bottom). Scans representing accumulation of intermediate product are shown on the left, while scans representing further consumption of the intermediate product are shown on the right.

TMB semiquinone−imine cation free radical (blue product) followed by the formation of yellow diimine product.[47] The appearance of the green color is simply due to the mixing of the initial blue product and the final yellow product. This result confirmed that the protein is still enzymatically active after encapsulation in the hydrogel. Importantly, the rate of the color change was different for the opposite parts of the hydrogel film. It was fastest in the region characterized by the highest content of the attached BP groups and the loaded enzyme (bottom part in the images of the hydrogel, Figure 5). On the contrary, the rate of enzymatic reaction in the opposite part of the hydrogel was lowest (upper part in the images of the hydrogel, Figure 5). Neither the outer solution color change nor the other visible evidence of hydrogel content release into the outer solution was observed during oxidation. Thus, it was concluded that the reaction took place exclusively inside the hydrogel.

We performed control cyt *c* catalyzed oxidation reactions in solution in order to determine factors that provided different rates of reaction in the parts of gradient hydrogel. The concentrations of TMB and hydrogen peroxide were set at 0.2 and 0.33 mg/mL, respectively. These concentrations were chosen to be close to the concentration of the reagents in the HABP hydrogel section after loading with TMB (see Supporting Information). Because HA matrix modified with a graded amount of BPs might have an impact on oxidation of TMB, the solution reactions were performed in the presence of either HA-hy or bisphosphonated HA (HA-BP) (concentration of the HA derivatives in the final reaction mixture was 2.67 mg/mL). HA-BP derivative was prepared from soluble thiolated HA by thiol−ene reaction in solution as previously described.[48] Optical spectroscopy study confirmed that the reaction clearly proceeded as two-electron oxidations (Figure 6). One-electron oxidation intermediate was initially being accumulated exhibiting an increase of absorbance at 653 nm (left spectra in Figure 6). After reaching a maximal value, it then started to decay and was replaced by a peak at 443 or 433 nm for the reaction with HA-hy or HA-BP, respectively (right spectra in Figure 6). This later stage was therefore characterized by a pair of isosbestic points on either side of the peak of the two-electron oxidation product in accordance to the literature.[47] It is worth noting that the rates of both stages of TMB oxidation were higher in the presence of HA-BP as compared to HA-hy despite the same cyt *c* concentration used (0.17 mg/mL). This impact of bisphosphonated HA on peroxidase activity of cyt *c* might be due to possible binding of anionic BP groups to ferri and ferro forms of the enzyme. For example, it was reported that inorganic orthophosphates enhanced the rate of electron transfer from ferrous ions to ferricytochrome *c*.[49] Because in our gradient hydrogel concentrations of both the matrix-linked BP groups and cyt *c* are increased in one direction, it may have an additive effect on the rate of TMB oxidation in the hydrogel. We increased the enzyme concentration to 0.5 mg/mL and observed that the time of reaching the maximal absorbance at 653 nm was decreased from 27.5 to 10 min in the reaction system containing HA-BP (Figure S10, Supporting Information). Consumption of the intermediate was also faster in this system. On the other hand, the reaction system containing HA-hy was mainly responsive to the change of enzyme

DOI: 10.1021/am506926w
ACS Appl. Mater. Interfaces 2015, 7, 1194−1206

concentration during the second-electron oxidation reaction. Clearly, different mechanisms might be in action for these systems, which requires additional investigation.

EXPERIMENTAL SECTION

Materials. Hyaluronic acid (HA) sodium salt (MW 150 kDa) was purchased from Lifecore Biomedical. 1-Ethyl-3-(3-(dimethylamino)-propyl) carbodiimide (EDC) and *N*-hydroxybenzotriazole (HOBt) were purchased from Fluka. Hyaluronidase (Hase), phosphate-buffered saline (PBS), and D,L-dithiothreitol (DTT) were purchased from Aldrich Chemical Co. Water-soluble initiator Irgacure 2959 was purchased from BASF Chemical Co. All solvents were of analytical quality (p.a.) and were dried over 4 Å molecular sieves. Alamar Blue was purchased from Invitrogen (Sweden). All other materials for cell cytotoxicity study were purchased from Sigma. Dialysis membranes Spectra/Por 6 (3500 g/mol cutoff) were purchased from VWR international. ^{1}H NMR spectra were recorded in D_2O with a JEOL JNM-ECP Series FT NMR spectrometer at a magnetic field strength 9.4 T, operating at 400 MHz. UV−vis absorption spectra were recorded using UV−vis spectrometer (Lambda 35, PerkinElmer Instruments). Fluorescence spectra were recorded on a LS 45 Luminescence Spectrometer (PerkinElmer Instruments).

Modification of HA Polymers. Details of the synthesis of all utilized HA derivatives is given in the Supporting Information. Briefly, hyaluronic acid has been modified with hydrazide and thiol groups using an orthogonal disulfide protecting group strategy as reported previously[35] affording HA-hy-SH. Hyaluronic acid modified with hydrazide groups (HA-hy) was prepared analogously using only one type of modifying reagent. HA derivatized with aldehyde groups (HA-al) was prepared according to our previous protocol.[50]

Preparation of Homogeneous Hydrogels. Irgacure 2959 initiator has been dissolved in degassed water at a concentration of 0.4% (4 mg/mL). HA-hy-SH (6 mg, 14.4 μmol of disaccharide units, 2.87 μmol of thiol groups, 1.435 μmol of hydrazide groups) was dissolved in 300 μL of the initiator solution. Separately, HA-al (6 mg, 15.5 μmol of disaccharide units, 1.435 μmol of aldehyde groups) was dissolved in 300 μL of the initiator solution. A specified amount (0−15 mg) of 3-(acrylamido-1-hydroxypropane-1,1-diyl)bis(phosphonic acid) (BP-acrylamide) was then dissolved in the HA-al solution. The two solutions of HA derivatives were mixed in an Eppendorf tube and immediately transferred into a 2 mL syringe. The syringe was sealed and left horizontally for hydrazone cross-linking of the gel content for 2 h. After hydrogel setting, it was carefully removed from the syringe and irradiated with UV light (36W UV timer lamp, CNC international BV, Netherlands) for 10 min. The hydrogel was then washed with 0.17 M NaCl solution (10 mL) for 4 h followed by repeated washing overnight.

Preparation of Gradient Hydrogels. Irgacure 2959 initiator has been dissolved in degassed water at a concentration of 0.4% (4 mg/mL). HA-SH-hy (6 mg, 14.4 μmol of disaccharide units, 2.87 μmol of thiol groups, 1.435 μmol of hydrazide groups) was dissolved in 300 μL of the initiator solution. Separately, HA-al (6 mg, 15.5 μmol of disaccharide units, 1.435 μmol of aldehyde groups) was dissolved in 300 μL of the initiator solution. The two solutions of HA derivatives were mixed in an Eppendorf tube and immediately transferred into a 2 mL syringe. The syringe was sealed and left horizontally for hydrazone cross-linking of the gel content for 2 h. After hydrogel setting, 200 μL of degassed water containing initiator (0.4%) and BP-acrylamide (9 mg, 31.1 μmol) was applied on top of the hydrogel and allowed to diffuse in for 2 h. The hydrogel was carefully removed from the syringe and irradiated with UV light for 10 min. The hydrogel was then washed with 0.17 M NaCl solution (10 mL) for 4 h followed by repeated washing overnight. The above procedure was modified in order to assess the influence of BP reagent, UV light, and matrix-immobilized thiol groups on the formation of gradients of BP groups in HA hydrogels. In particular, 200 μL of degassed water containing only initiator (0.4%) was applied to diffuse through HA matrix to obtain noBP hydrogel. A hydrogel was directly soaked in 0.17 M NaCl solution after diffusion step without UV light treatment to obtain noUV hydrogel. Finally, HA-hy derivative (6 mg) was used instead of HA-SH-hy to obtain noSH hydrogel (both derivatives were characterized by the same 10% of modification with hydrazide groups).

Characterization of Gradient Hydrogels. Gradient hydrogels (n = 3) after preparation and purification were cut perpendicularly to the diffusion axis into four sections of equal thickness (Figure S1b, Supporting Information). The sections were freeze dried, and phosphorus in different sections was verified by SEM-energy-dispersive X-ray spectroscopy (SEM-EDXS). Acc. voltage was 5 keV.

Biomineralization of Gradient Hydrogels. Gradient hydrogels after preparation and purification were placed into simulated body fluid (SBF, 5 mL) for 1 h, 1 day, or 7 days. After incubation in SBF, the samples were washed with 5 mL of deionized water (3 × 15 min) to remove unbound ions from the gel samples. Hydrogels were cut perpendicularly to the diffusion axis into four sections of equal thickness (Figure S1b, Supporting Information). The sections were freeze dried. Freeze-dried samples were incubated in 0.5 M acetic acid (1 mL). A 200 μL amount from each sample solution was diluted with 5.4 mL of 0.4 mM Arsenazo III in 10 mM Hepes buffer. pH was adjusted to 7.4 by addition of 220 μL of 5 M NaOH, and the resulting 5.82 mL of neutral solution was further filled up until 6 mL with 0.4 mM Arsenazo III in Hepes buffer. Three milliliter aliquots from the samples treated with calcium-sensitive dye were taken for calcium determination (UV absorbance was measured at 650 nm). The mass of deposited Ca^{2+} was calculated according to the following equation

$$m = M(Ca^{2+}) \times V/200\mu L \times c \times 0.006$$

where V (μL) is the volume of liquid obtained after extraction of freeze-dried hydrogel with 1 mL of 0.5 M acetic acid, $M(Ca^{2+})$ is the atomic mass of calcium (= 40 μg/μmol), and c is the concentration of calcium in the measured sample and determined using the calibration curve for $CaCl_2$ solutions (Supporting Information, Figure S7). The number of examined samples was 3 per group.

Loading of Cytochrome *c* to Hydrogels. Hydrogels after washing in 0.17 M NaCl solution were placed in PBS (5 mL) containing cyt *c* at 1 mg/mL concentration for 5 days.

Mechanical Properties of Hydrogels. Rheological characterization of all hydrogels were performed using an AR2000 Advanced Rheometer (TA Instruments) with an aluminum parallel plate geometry of 8 mm diameter. Frequency sweeps from 0.1 to 10 Hz were performed by monitoring storage (G') and loss moduli (G'') at a fixed normal force (0.015 N) and a fixed strain. All experiments were repeated three times.

Release of Cytochrome *c* from Homogeneous Hydrogels. Homogeneous hydrogels with loaded cyt *c* were divided into two approximately equal parts. One part was incubated overnight in 1.5 mL of PBS containing hyaluronidase at 1 mg/mL concentration. The amount of the protein in the degraded hydrogel was determined by UV−vis spectrophotometry using the calibration curve for cyt *c* solutions (Supporting Information, Figure S5). Another part was incubated in free PBS (3 mL). After certain intervals of time (1, 2, 4, 22, 48, 97, 169, 241, and 317 h), PBS buffer was withdrawn and replaced with the fresh one. The collected release samples were examined by UV−vis spectrophotometry (UV absorbance was measured at 410 nm).

Determination of Cytochrome *c* Loaded in Gradient Hydrogels. Cyt *c* loaded gradient hydrogels were cut perpendicularly to the axis of diffusion of BP-acrylamide reagent into four sections of equal thickness. Each section was incubated overnight in 1 mL of PBS containing hyaluronidase at 1 mg/mL concentration. Digests were filtered through a cotton plug to remove remained hydrogel debris, and the amount of cyt *c* in the filtered digests was determined by UV−vis spectrophotometry.

Release of Cytochrome *c* from Sections of Gradient Hydrogels. Cyt *c* loaded gradient hydrogels were cut perpendicularly to the axis of diffusion of BP-acrylamide reagent into four sections of equal thickness. The sections were incubated in PBS (1.5 mL) for 24 h. The release medium from each release sample was diluted with 1.5 mL of fresh PBS, and UV−vis absorbance was measured at 410 nm. The remaining gels were degraded in 1.5 mL of PBS containing

DOI: 10.1021/am506926w
ACS Appl. Mater. Interfaces 2015, 7, 1194−1206

hyaluronidase at 1 mg/mL concentration. The degraded medium from each gel sample was diluted with 1.5 mL of fresh PBS, and UV−vis absorbance was also measured.

Cytotoxicity Study. MCF-7 cells were cultured in DMEM (Sigma) with 10% FBS (Hyclone) and 1% Pen/Strep (Hyclone) until they become confluent. Cells were passaged three times before the assay. Cells were then trypsinized and plated at 40 000 cells/well in a 24-well plate. At 24 h, the cells were washed with 1 × PBS and sections from gradient hydrogel were placed into cell culture inserts. The inserts were placed into the wells containing the cells in 5% DMEM (1.5 mL) for 24 h. After 24 h of incubation, the insets were removed and the gel samples were preserved for further analysis. The medium in the wells was removed, and the cells were washed once with 1 × PBS to remove any traces of cyt *c*. Fresh medium containing 10% Alamar Blue was added into the wells, and the cells were placed into an incubator at 37 °C and 5% CO_2 for 3 h. Aliquots of the medium were subsequently transferred in triplicate to a 96-well plate, and fluorescence was measured (excitation and emission wavelengths were 570 and 590 nm, respectively). The obtained values were averaged and normalized against controls.

Oxidation of TMB in Cytochrome *c* Loaded Gradient HABP Hydrogel. Cyt *c* loaded gradient hydrogel (664.5 mg) was sectioned along the axis of diffusion of BP-acrylamide reagent to obtain a 1 mm thick hydrogel film with a mass of 165.9 mg (Figure S8, Supporting Information). A 1 mg amount of 3,3′,5,5′-tetramethylbenzydine (TMB) was dissolved in 0.5 mL of DMSO, and the solution was diluted with 4.5 mL of water. The middle film section of the cyt *c* loaded hydrogel was incubated in 5 mL of TMB solution for 2 h. TMB solution (4.57 mL) was then removed, and the gel section (386 mg) was placed into 10 mL of water containing 2 μL of H_2O_2. The change of color in the gel was monitored for 100 min, while the whole time of incubation was 23 h.

CONCLUSIONS

In this work we showed that long-range stable gradients of physically immobilized molecules within a hydrogel matrix can be obtained by diffusion of an acrylamide reagent through a thiol-presenting matrix. An established physical gradient pattern can be determined by the geometry of the mold used and the site of application of the solution of acrylamide derivative(s). The physical gradient was subsequently stabilized in the course of "click"-type UV-light-triggered thiol−ene addition reaction. This strategy was validated for the gradient 3D immobilization of bisphosphonates in hyaluronic acid hydrogel by orthogonal combination of hydrazone cross-linking with thiol−ene photoaddition reactions in a sequential manner without any intermediate purification steps. Bisphosphonates were subsequently functioning as affinity groups for secondary immobilization of positively charged cytochrome *c* which transformed the gradient of chemically linked molecules into a gradient of proteins bound via Coulombic interactions. Gradient loading of the protein resulted in its gradient release with both highest release of absolute amount and highest relative retention of cyt *c* occurring from the most bisphosphonated area of the hydrogel. Such gradient release of cyt *c* led to the induction of gradient cytotoxicity to the surrounding cancer cells. The chemical gradient of BP groups within the HA matrix was also shown to induce a gradient biomineralization pattern in the hydrogel. Finally, gradient HABP hydrogel loaded with cyt *c* represented an enzymatic reactor in which oxidative conversion of TMB occurred with different rates within the reactor. Altogether, this study presents a synthetic strategy to hydrogels in which the hydrogel microenvironment is dynamically and gradually regulated in space.

ASSOCIATED CONTENT

Supporting Information

Synthesis procedures for BP-acrylamide, HA-al, HA-hy-SH, and HA-hy; NMR spectra of HA-hy-SH; images of gradient hydrogels; correlation between BP-acrylamide in feed and the amount of absorbed cyt *c*; standard UV−vis calibration curves for cyt *c*, $CaCl_2$, and TMB; sectioning of the cyt *c* loaded gradient HABP hydrogel; time-dependent UV−vis absorbance changes for enzymatic oxidation of TMB in solution; tables of phosphorus content of gradient HABP and hydrogel rheological properties of hydrogels. This material is available free of charge via the Internet at http://pubs.acs.org.

AUTHOR INFORMATION

Corresponding Author

*E-mail: dmitri.ossipov@kemi.uu.se.

Author Contributions

The manuscript was written through contributions of all authors. All authors have given approval to the final version of the manuscript.

Notes

The authors declare no competing financial interest.

ACKNOWLEDGMENTS

This work was supported by the European Community's Seventh Framework Programme (Biodesign project). We also thank Gradientech Co. whose CellDirector 3D product inspired us to perform this work.

REFERENCES

(1) Ulijn, R. V.; Bibi, N.; Jayawarna, V.; Thornton, P. D.; Todd, S. J.; Mart, R. J.; Smith, A. M.; Gough, J. E. Bioresponsive Hydrogels. *Mater. Today* **2007**, *10*, 40−48.

(2) Lutolf, M. P.; Hubbell, J. A. Synthetic Biomaterials as Instructive Extracellular Microenvironments for Morphogenesis in Tissue Engineering. *Nat. Biotechnol.* **2005**, *23*, 47−55.

(3) Burdick, J. A.; Murphy, W. L. Moving from Static to Dynamic Complexity in Hydrogel Design. *Nat. Commun.*, **2012**, *3*, doi: 10.1038/ncomms2271.

(4) Gjorevski, N.; Nelson, C. M. Bidirectional Extracellular Matrix Signaling During Tissue Morphogenesis. *Cytokine Growth Factor Rev.* **2009**, *20*, 459−465.

(5) DeForest, C. M.; Polizzoti, B. D.; Anseth, K. S. Sequential Click Reactions for Synthesizing and Patterning Three-dimensional Cell Microenvironments. *Nat. Mater.* **2009**, *8*, 659−664.

(6) Luo, Y.; Shoichet, M. S. A Photolabile Hydrogel for Guided Three-dimensional Cell Growth and Migration. *Nat. Mater.* **2004**, *3*, 249−253.

(7) Wylie, R. G.; Ahsan, S.; Aizawa, Y.; Maxwell, K. L.; Morshead, C. M.; Shoichet, M. S. Spatially Controlled Simultaneous Patterning of Multiple Growth Factors in Three-dimensional Hydrogels. *Nat. Mater.* **2011**, *10*, 799−806.

(8) Mosiewicz, K. A.; Kolb, L.; van der Vlies, A. J.; Martino, M. M.; Lienemann, P. S.; Hubbell, J. A.; Ehrbar, M.; Lutolf, M. P. In Situ Cell Manipulation Through Enzymatic Hydrogel Photopatterning. *Nat. Mater.* **2013**, *12*, 1072−1078.

(9) DeForest, C. A.; Anseth, K. S. Cytocompatible Click-based Hydrogels with Dynamically-Tunable Properties Through Orthogonal Photoconjugation and Photocleavage Reactions. *Nat. Chem.* **2011**, *3*, 925−931.

(10) Griffin, D. R.; Kasko, A. M. Photodegradable Macromers and Hydrogels for Live Cell Encapsulation and Release. *J. Am. Chem. Soc.* **2012**, *134*, 13103−13107.

(11) Komatsu, H.; Tsukiji, S.; Ikeda, M.; Hamachi, I. Stiff, Multistimuli-Responsive Supramolecular Hydrogels as Unique Molds

DOI: 10.1021/am506926w
ACS Appl. Mater. Interfaces 2015, 7, 1194−1206

for 2D/3D Microarchitectures of Live Cells. *Chem.—Asian J.* **2011**, *6*, 2368−2375.
(12) Shamloo, A.; Ma, N.; Poo, M.; Sohn, L. L.; Heishorn, S. C. Endothelial Cell Polarization and Chemotaxis in a Microfluidic Device. *Lab Chip* **2008**, *8*, 1292−1299.
(13) Chung, S.; Sudo, R.; Vickerman, V.; Zervantonakis, I. K.; Kamm, R. D. Microfluidic Platforms for Studies of Angiogenesis, Cell Migration, and Cell-Cell Interactions. *Ann. Biomed. Eng.* **2010**, *38*, 1164−1177.
(14) Vogel, V.; Sheetz, M. Local Force and Geometry Sensing Regulate Cell Functions. *Nat. Rev. Mol. Cell Biol.* **2006**, *7*, 265−275.
(15) Yang, P. J.; Temenoff, J. S. Engineering Orthopedic Tissue Interfaces. *Tissue Eng., Part B Rev.* **2009**, *15*, 127−141.
(16) Sant, S.; Hancock, M. J.; Donnely, J. P.; Iyer, D.; Khademhosseini, A. Biomimetic Gradient Hydrogels for Tissue Engineering. *Can. J. Chem. Eng.* **2010**, *88*, 899−911.
(17) Fox, J. D.; Capadona, J. R.; Marasco, P. D.; Rowan, S. J. Bioinspired Water-Enhanced Mechanical Gradient Nanocomposite Films that Mimic the Architecture and Properties of the Squid Beak. *J. Am. Chem. Soc.* **2013**, *135*, 5167−5174.
(18) Wong, J. Y.; Velasco, A.; Rajagopalan, P.; Pham, Q. Directed Movement of Vascular Smooth Muscle Cells on Gradient-Compliant Hydrogels. *Langmuir* **2003**, *19*, 1908−1913.
(19) Nemir, S.; Hayenga, H. N.; West, J. L. PEGDA Hydrogels with Patterned Elasticity: Novel Tools for the Study of Cell Response to Substrate Rigidity. *Biotechnol. Bioeng.* **2010**, *105*, 636−644.
(20) Kloxin, A. M.; Benton, J. A.; Anseth, K. S. In Situ Elasticity Modulation with Dynamic Substrates to Direct Cell Phenotype. *Biomaterials* **2010**, *31*, 1−8.
(21) Marklein, R. A.; Burdick, J. A. Spatially Controlled Hydrogel Mechanics to Modulate Stem Cell Interactions. *Soft Matter* **2010**, *6*, 136−143.
(22) Aizawa, Y.; Wylie, R.; Shoichet, M. S. Endothelial Cell Guidance in 3D Patterned Scaffolds. *Adv. Mater.* **2010**, *22*, 4831−4835.
(23) Hahn, M. S.; Miller, J. S.; West, J. L. Three-Dimensional Biochemical and Biomechanical Patterning of Hydrogels for Guiding Cell Behavior. *Adv. Mater.* **2006**, *18*, 2679−2684.
(24) Vepari, C. P.; Kaplan, D. L. Covalently Immobilized Enzyme Gradients within Three-Dimensional Porous Scaffolds. *Biotechnol. Bioeng.* **2006**, *93*, 1130−1137.
(25) van Beek, E.; Hoekstra, M.; van de Ruit, M.; Lowik, C.; Papapoulos, S. Structural Requirements for Bisphosphonate Actions In Vitro. *J. Bone Miner. Res.* **1994**, *9*, 1875−1882.
(26) Russell, R. G.; Watts, N. B.; Ebetino, F. H.; Rogers, M. J. Mechanisms of Action of Bisphosphonates: Similarities and Differences and Their Potential Influence on Clinical Efficacy. *Osteoporosis Int.* **2008**, *19*, 733−759.
(27) Martin de Rosales, R. T.; Finucane, C.; Foster, J.; Mather, S. J.; Blower, P. J. $^{188}Re(CO)_3$-Dipicolylamine-Alendronate: A New Bisphosphonate Conjugate for the Radiotherapy of Bone Metastases. *Bioconjugate Chem.* **2010**, *21*, 811−815.
(28) Erez, R.; Ebner, S.; Attali, B.; Shabat, D. Chemotherapeutic Bone-Targeted Bisphosphonate Prodrugs with Hydrolytic Mode of Activation. *Bioorg. Med. Chem. Lett.* **2008**, *18*, 816−820.
(29) Wright, J. E. I.; Gittensb, S. A.; Bansala, G.; Kitovd, P. I.; Sindreye, D.; Kucharskia, C.; Uludag, H. A Comparison of Mineral Affinity of Bisphosphonate-Protein Conjugates Constructed with Disulfide and Thioether Linkages. *Biomaterials* **2006**, *27*, 769−784.
(30) Low, S. A.; Kopeček, J. Targeting Polymer Therapeutics to Bone. *Adv. Drug Delivery Rev.* **2012**, *64*, 1189−1204.
(31) Renner, C.; Piehler, J.; Schrader, T. Arginine- and Lysine-Specific Polymers for Protein Recognition and Immobilization. *J. Am. Chem. Soc.* **2006**, *128*, 620−628.
(32) Hulsart-Billström, G.; Yuen, P. K.; Marsell, R.; Hilborn, J.; Larsson, S.; Ossipov, D. Bisphosphonate-Linked Hyaluronic Acid Hydrogel Sequesters and Enzymatically Releases Active Bone Morphogenetic Protein-2 for Induction of Osteogenic Differentiation. *Biomacromolecules* **2013**, *46*, 3055−3063.
(33) Bertini, I.; Cavallaro, G.; Rossato, A. Cytochrome C: Occurence and Functions. *Chem. Rev.* **2006**, *106*, 90−115.
(34) Hengartner, M. O. The Biochemistry of Apoptosis. *Nature* **2000**, *407*, 770−776.
(35) Ossipov, D. A.; Yang, X.; Varghese, O.; Kootala, S.; Hilborn, J. Modular Approach to Functional Hyaluronic Acid Hydrogels Using Orthogonal Chemical Reactions. *Chem. Commun.* **2010**, *46*, 8368−8370.
(36) Dumetz, A. C.; Snellinger-O'Brien, A. M.; Kaler, E. W.; Lenhoff, A. M. Patterns of Protein-Protein Interactions in Salt Solutions and Implications for Protein Crystallization. *Protein Sci.* **2007**, *16*, 1867−1877.
(37) Tseng, H.; Puperi, D. S.; Kim, E. J.; Ayoub, S.; Shah, J. V.; Cuchiara, M. L.; West, J. L.; Grande-Allen, K. J. Anisotropic Poly(Ethylene Glycol)/Polycaprolactone Hydrogel-Fiber Composites for Heart Valve Tissue Engineering. *Tissue Eng., Part A* **2014**, *20*, 2634−2645.
(38) Oh, K. T.; Bronich, T. K.; Kabanov, V. A.; Kabanov, A. V. Block Polyelectrolyte Networks from Poly(acrylic acid) and Poly(ethylene oxide): Sorption and Release of Cytochrome C. *Biomacromolecules* **2007**, *8*, 490−497.
(39) Cramer, N. B.; Davies, T.; O'Brien, A. K.; Bowman, C. N. Mechanism and Modeling of a Thiol-Ene Photopolymerization. *Macromolecules* **2003**, *36*, 4631−4636.
(40) Reddy, S. K.; Okay, O.; Bowman, C. N. Network Development in Mixed Step-Chain Growth Thiol-Vinyl Photopolymerizations. *Macromolecules* **2006**, *39*, 8832−8843.
(41) Wang, L.; Zhang, M.; Yang, Z.; Xu, B. The First Pamidronate Containing Polymer and Copolymer. *Chem. Commun.* **2006**, *26*, 2795−2797.
(42) Lemberg, R.; Barrett, J. *Cytochromes*, 1st ed.; Academic Press: London, 1973; pp 122−216.
(43) Yang, X.; Akhtar, S.; Rubino, S.; Leifer, K.; Hilborn, J.; Ossipov, D. Direct "Click" Synthesis of Hybrid Bisphosphonate-Hyaluronic Acid Hydrogel in Aqueous Solution for Biomineralization. *Chem. Mater.* **2012**, *24*, 1690−1697.
(44) Crouzier, T.; Szarpak, A.; Boudou, T.; Auzély-Velty, R.; Picart, C. Polysaccharide-Blend Multilayers Containing Hyaluronan and heparin as a Delivery System for rhBMP-2. *Small* **2010**, *6*, 651−662.
(45) Bongio, M.; Nejadnik, M. R.; Birgani, T.; Habibovic, P.; Kinard, L. A.; Kasper, K.; Mikos, A. G.; Jansen, J. A.; Leeuwenburgh, S. C. G.; van den Beucken, J. J. P. In Vitro and In Vivo Enzyme-Mediated Biomineralization of Oligo(poly(ethylene glycol) Fumarate Hydrogels. *Macromol. Biosci.* **2013**, *13*, 777−788.
(46) Fejerskov, B.; Jensen, N. B. S.; Teo, B. M.; Städler, B.; Zelikin, A. N. Byocatalytic Polymer Coatings: On-Demand Drug Synthesis and Localized Therapeutic Effect under Dynamic Cell Culture Conditions. *Small* **2014**, *10*, 1314−1324.
(47) Josephy, P. D.; Eling, T.; Mason, R. P. The Horseradish Peroxidase-Catalyzed Oxidation of 3,5,3′,5′-Tetramethylbenzidine. Free Radical and Charge-Transfer Complex Intermediates. *J. Biol. Chem.* **1982**, *257*, 3669−3675.
(48) Nejadnik, M. R.; Yang, X.; Bongio, M.; Alghamdi, H.; van den Beucken, J.; Huysmans, M.; Jansen, J.; Hilborn, J.; Ossipov, D.; Leeuwenburgh, S. C. G. Self-Healing Hybrid Nanocomposites Consisting of Bisphosphonated Hyaluronan and Calcium Phosphate Nanoparticles. *Biomaterials* **2014**, *35*, 6918−6929.
(49) Taborsky, G. Phosphate Binding by Cytochrome C. *J. Biol. Chem.* **1979**, *254*, 5246−5251.
(50) Ossipov, D. A.; Piskounova, S.; Varghese, O. P.; Hilborn, J. Functionalization of Hyaluronic Acid with Chemoselective Groups via a Disulfide-Based Protection Strategy for In Situ Formation of Mechanically Stable Hydrogels. *Biomacromolecules* **2010**, *11*, 2247−2254.

DOI: 10.1021/am506926w
ACS Appl. Mater. Interfaces 2015, 7, 1194−1206